P3.9

THE SEASONAL CYCLE OF WILDFIRE AND CLIMATE IN THE WESTERN UNITED STATES

P.J. Bartlein[1*], S.W. Hostetler[2], S.L. Shafer[2], J.O. Holman[1], and A.M. Solomon[3]

[1] Department of Geography, University of Oregon, Eugene OR
[2] U.S. Geological Survey, Corvallis OR
[3] U.S. Environmental Protection Agency, Corvallis OR

1. INTRODUCTION

The incidence of wildfire in the western United States displays a strong seasonal cycle, related to climatically driven cycles of flammability and ignition. We illustrate here the seasonal cycle of wildfire and climate in the western United States using a combination of observed and simulated climate data sets, along with a daily data set consisting of the point locations of individual fires.

Following several months of decreasing soil moisture across the region, fires started by all ignition sources reach their annual maximum in the first half of August during a time of frequent thunderstorms and generally low precipitation. There is a distinct spatial pattern in the incidence of fire across the western U.S.: the peak season occurs earlier in the southwest, progresses to the interior deserts and mountains, Pacific Northwest and Northern Rocky Mountains, and occurs later in the Mediterranean ecosystems of California. This pattern of fire incidence reflects the seasonal variations of soil moisture, which in turn are controlled by the seasonal variations of the surface energy budget that are driven by insolation and precipitation.

2. DATA SETS AND SOURCES

2.1 *Fire-Start and Ecoregion Data*

We used daily fire-start data from the 1986-1996 National Fire Occurrence data base as described in Hardy et al. (2001, *Intl. J. Wildland Fire* 10:353-372; available at http://www.fs.fed.us/fire/fuelman/). These data consist of the locations of individual fires, the date when each was first reported, and for most records, the ultimate size of the fire and the date when it was considered controlled (but not necessarily extinguished). A subset of the data was extracted that contains 332,404 records from west of 102°W. Further discussion of the nature of these daily fire-start records can be found in Hardy et al. (2001), the review by Westerling et al. (2003), and in an assessment of the quality of such data by Brown et al. (2002). These data are not without problems, but we believe that they are sufficient for our purposes here. One obvious limitation of the data set is the relatively short record (11 years). This situation raises the possibility that the specific patterns revealed by the data could be overly influenced by interannual variations of fire incidence and climate, if one or more unusual years came to dominate the patterns. Inspection of the data suggests, however, that there is broad year-to-year similarity in the distribution of fires; individual years differ mainly in the number of fires in a way that is consistent with the interannual variations of climate. Subsets of data were created that include all fires started by lighting and all fires started by humans. We did not grid the data, preferring to retain the informative spatial variability of the point-location data.

In order to gain insight on the broad-scale influence of vegetation on the seasonal cycle of fire incidence, we classified each record biogeographically according to the specific “ecoregion province”

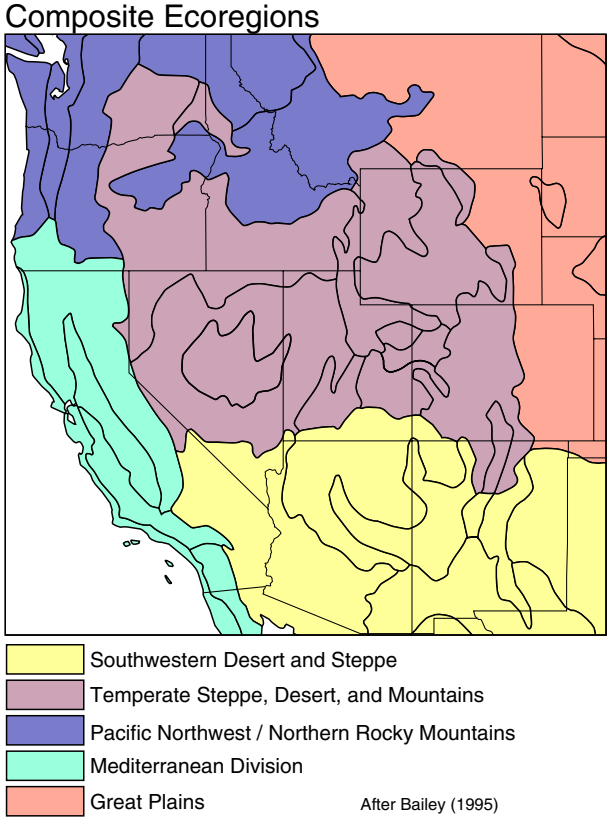

Figure 1: Composite ecoregions used to summarize the fire-start data. The component ecoregion provinces of Bailey (1995) are also shown.

*Corresponding author address: Patrick J. Bartlein, Department of Geography, University of Oregon, 1251 Univ. Oregon, Eugene OR, 97403-1251;
email: bartlein@uoregon.edu

in which it occurs (Bailey, 1995). Based on a preliminary analysis of the fire-start data classified by ecoregion provinces and divisions, we constructed five composite ecoregions that will be used in characterizing the data here (Fig. 1).

2.2 *Climate Data*

The average seasonal cycle of climate was characterized using a combination of observed and simulated variables. Observed temperature and precipitation were described using the "CRU TS 2.0" data set (Mitchell et al. 2003), a global, 0.5-degree gridded data set (for land points only), that spans the interval 1901-2000. We used this data set because it allowed us to calculate "long-term" means for the specific interval represented by the fire data (1986-1996), and because the interpolation inherent in its creation provides data for regions where individual climate stations are sparse.

We examined soil moisture as an index of the potential flammability of both dead and live fuel moisture, following other studies that have shown a linkage between surficial hydrologic drought indicators and fire incidence (Swetnam and Betancourt 1998; Westerling et al 2003). Soil moisture was calculated as part of simulations performed with a regional climate model, modified from RegCM2 (Giorgi et al. 1993), that we ran for the period 1978-2002 using data from the NCEP/NCAR Reanalysis Project data (Kistler et al. 2001) to provide lateral boundary conditions at 6-hour intervals. The specific implementation of RegCM2 used here is coupled with the LSX land-surface physics package (Thompson and Pollard 1995), and the spacing of the model grid points here is 45km, roughly similar to the resolution of the CRU data. Details of the application of the model can be found in Hostetler et al. (2003). The total moisture content in the top 5cm is expressed as a percentage of saturation of that layer.

Temperature, precipitation and soil moisture were also expressed as intermonthly changes in the long-term means. This manner of displaying the data clearly illustrates the month-to-month changes in the values of the different variables, while also diminishing the strong effect of elevation on temperature and precipitation that otherwise would be present in the raw monthly values (Mock, 1995).

3. RESULTS AND DISCUSSION

3.1 *Seasonal cycles of lightning-started, human-started, and all fires*

The total number of fires from all ignition sources for each day of the year, plotted as a function of day number, resembles a Gaussian curve that reaches an annual maximum during the first half of August (Fig. 2). Fires started by lightning are almost entirely restricted to the interval from late April through October, while those started by human causes occur during any month of the year.

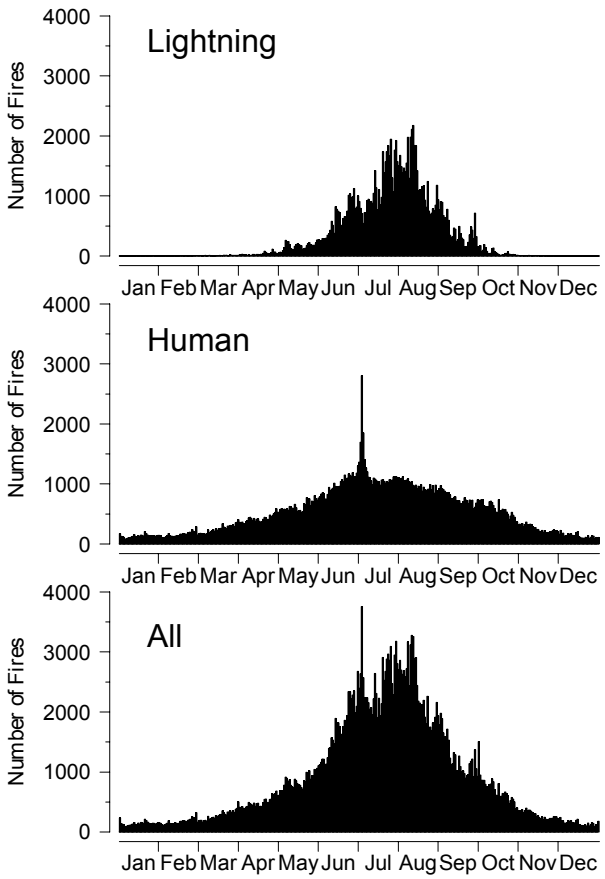

Figure 2: The total number (1986-1996) of fires started by lighting (top), humans (middle) and from all ignition sources (bottom) for each day of the year, plotted as a function of day number.

There is a prominent singularity in the frequency of human-started fires around the Fourth of July, when daily fire frequencies attain levels three times higher than those just before or after the holiday. High summertime levels of human-started fires tend to taper off gradually during the autumn, with a slight shoulder in the distribution marking the end of the outdoor-recreation season at the end of October. In general, the shape of the distribution of the total number of fires resembles that of the lightning-started fires more than that of the human-started fires; the latter act mainly to determine the shape of the distribution of all fires during the late autumn, winter, and early spring. Despite the large number of human-started fires, the variation in the total number of fires during the summer is strongly modulated by the number of lightning-started fires.

3.2 *Variations in the incidence of fires by ecoregion*

The time of year of peak incidence of fires from all sources varies both across the western U.S. and among ecoregions. Figure 3 shows the distributions of fires for the five composite ecoregions, arranged by the date of the lightning-started fire maximum,

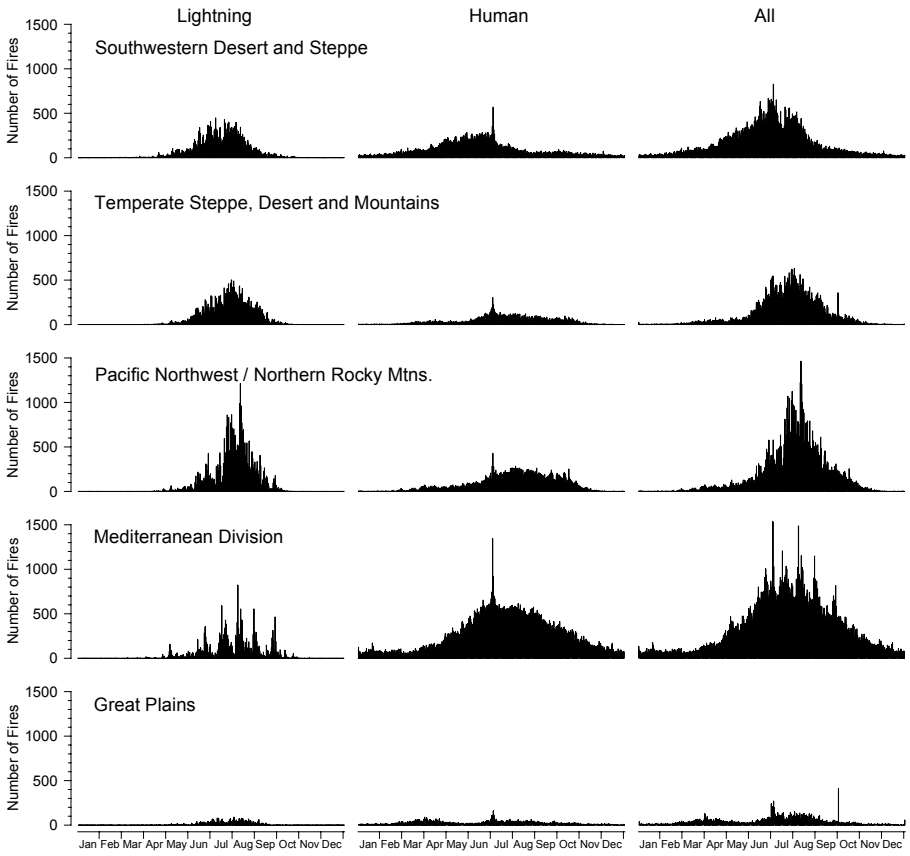

Figure 3: The total number (1986-1996) of fires started by lighting (top), humans (middle) and from all ignition sources (bottom) for each day of the year, plotted as a function of day number and composite ecosystem

and Fig. 4 shows the point locations of the lightning- and human-started fires.

Fires occur earlier in the southwestern desert and steppe composite ecoregions (SW), and progress, in order, into the intermountain west and southern Rocky Mountains (the Temperate Steppe, Desert and Mountains composite ecoregion (TSDM)), the Pacific Northwest and northern Rocky Mountains (PNW & NRM), and California (i.e. the Mediterranean Division (MD) composite ecoregion). Wintertime fires in the western U.S. are almost exclusively restricted to the MD region. Human-started fires in the MD region increase in number earlier in the year than in the PNW & NRM region, reflecting the generally drier conditions and larger populations there.

With the exception of the Mediterranean Division (MD), the timing of the peak number of human-started fires and fires from all sources follow the progression of lightning-started fires. The very small number of fires in the Great Plains (GP) composite ecoregion is an artifact of the fire-reporting process for non-federal lands (Westerling et al. 2003; Brown et al. 2002), and represents severe underreporting of fires there.

3.3 *The seasonal cycles of climate variables*

The seasonal cycles of different climate variables in the western U.S. reflect the direct effects of insolation on surface water and energy balances, along with the indirect effects of insolation on atmospheric circulation, and hence precipitation. The seasonal cycle of temperature (Fig. 4) clearly expresses the insolation effect, but also illustrates the thermal inertia of the oceans and their influence on terrestrial climate. Monthly mean temperatures peak in July (and in some locations, August), after the summer solstice, and intermonthly changes in temperature are greatest in the continental interior, and least along the west coast. The effects of elevation on temperature are clearly apparent throughout the year: month-to-month increases in temperature in spring in high-elevation areas remain relatively small until winter snowpack has melted.

The seasonal cycle of precipitation reflects the antiphasing of two dominant atmospheric circulation features that are driven by the seasonal cycle of insolation. The first mechanism, the midlatitude westerlies, are strongest and farthest south during the winter, when the latitudinal temperature gradient is steepest, and the circumpolar vortex is at its greatest extent. Storm systems frequently form in the Gulf of Alaska in winter and move onshore, providing support for precipitation derived ultimately from moisture from subtropical Pacific sources. Precipitation is greatest in winter along

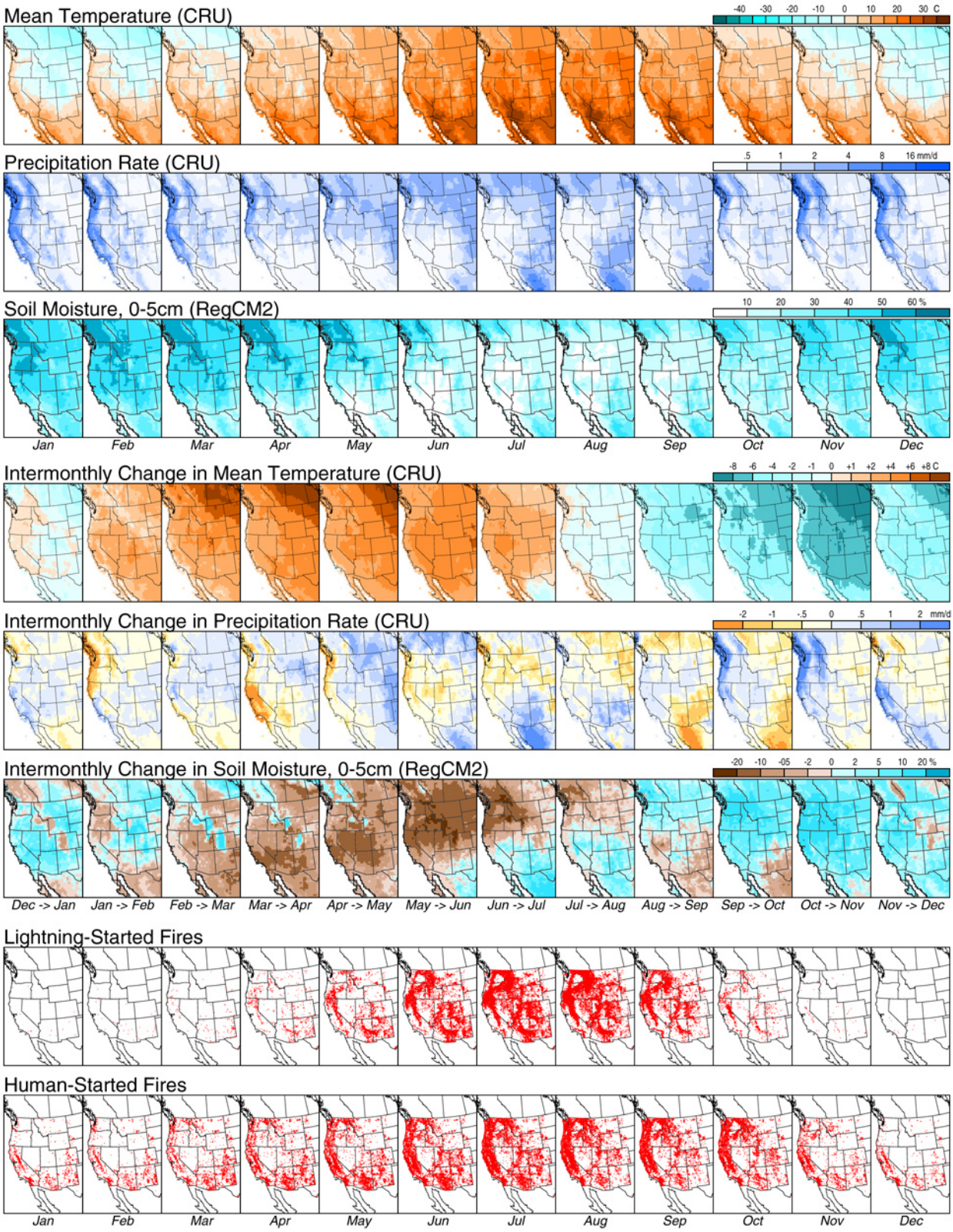

Figure 4. Seasonal cycles of climate variables and point locations of lightning- and human-started fires. CRU indicates data from Mitchell et al. (2003), and RegCM2 denotes data from our regional climate-model simulations. The fire-start locations are from Hardy et al. (2001). Intermonthly changes are the values of the long-term mean for the current month, minus those for the previous month.

the west coast, and in higher-elevation areas in the interior, where it accumulates in winter snow pack. From winter into spring and summer, the westerlies retreat poleward as the temperature gradient is diminished, so that in summer (June, July, and August), westerly-derived precipitation is confined to Canada.

The second precipitation mechanism is the southwestern or Mexican monsoon, which is driven by differential heating of the continent and ocean in the summer, which generates low pressure over the continent, high pressure over the oceans, and consequent onshore flow of subtropical-Pacific moisture into the southern and southeastern part of the region, from May through August (Fig. 4). A second monsoon-like surge of moisture from the Gulf of Mexico in spring is evident along the eastern edge of the region mapped in Fig. 4.

The interplay between these two circulation systems generates patterns in the intermonthly changes in precipitation that are more complicated than those of temperature. The equatorward advance of the westerlies is quite evident in the month-to-month increases in precipitation along the west coast from September through December, while the subsequent retreat from January through July is more gradual. In contrast, the southwestern monsoon builds from May into August, but then diminishes rapidly in September and October. The intermonthly changes in precipitation throughout the year exhibit some form of opposition between the Pacific Northwest and Southwest, a pattern that can be amplified or damped by interannual climate variations, like those associated with ENSO.

Soil moisture variations throughout the year reflect the tradeoff between moisture supply from precipitation and snowmelt, and evaporative demand, driven by net radiation, and hence ultimately by insolation. Soil moisture is generally high throughout the region in winter, and in the southeastern part of the region in summer. The relative importance of the supply and demand components of soil moisture can be inferred from the intermonthly changes. In general, the intermonthly change patterns of soil moisture are of large spatial scale, resembling the scale (but not necessarily the pattern) of the intermonthly changes in temperature more than those of precipitation; this suggests a stronger effect on soil moisture of net radiation (to which temperature is related) than of precipitation. Superimposed on the broadscale patterns of intermonthly changes in soil moisture are smaller regions with changes opposite in sign to the broadscale changes. This scale of features is particularly evident in winter and spring; whereas in winter, below-freezing temperatures in upland areas result in the storage of moisture in snowpack and decreasing soil moisture (as is evident in the December to January intermonthly change), in spring this stored moisture replenishes soil moisture as can be seen in the February-to-March intermonthly change.

3.4 *Soil moisture and fire incidence*

The general patterns of soil moisture variations and their intermonthly changes throughout the year provide an explanation for the distribution of human-started fires relative to lightning-started ones, and for the temporal progression of higher levels of fire incidence from ecoregion to ecoregion (Fig. 3). Human-started fires, which occur at low but still substantial levels throughout the cool season (October to April), are generally confined to the regions of lowest soil moisture during this interval. Increases in human-started fires from February through April across the region (and in particular in southern California, Arizona, New Mexico and southern Colorado) correspond to areas of generally decreasing soil moisture over this interval. In some areas, such as New Mexico and Colorado, precipitation increases from March through May, while soil moisture continues to decrease, reflecting the growing evaporative demand during spring.

The general progression of the region of highest incidence of both lightning- and human-started fires from the SW composite ecoregion to the PNW & NRM ecoregion can be seen to track the area in which average soil moisture levels fall continuously over a two-to-three month period. A continuation of a high incidence of lightning-started fires in the SW in July and August despite increasing soil moisture can be explained by the frequent occurrence of monsoon-generated thunderstorms during those months; human-started fires abruptly decrease in frequency in July and August in that region. The end of the lighting-started fire season, and the decrease in the rate of human-started fires in October accompanies the general increase in soil moisture across the region in autumn, as winter precipitation commences and evaporative demand falls.

4. CONCLUSIONS

The incidence of fire in the western U.S. has a strong seasonal cycle, related to the seasonal cycles of the climatic mechanisms responsible for ignition and flammability of fuels. Examination of the daily record of fires over the interval 1986-1996 (Hardy et al. 2001) reveals:

- the overall pattern of fire initiation over the year is dominated by the summer maximum in lightning-started fires;
- human-started fires are frequent throughout the year, with a broad summertime maximum that reinforces that of lightning-started fires;
- a remarkable singularity in human-started fires occurs around the Fourth of July, in which human-started fires are three times more frequent than just before or after the holiday; and
- a regular spatial pattern in the timing of maximum incidence of fire exists, beginning earlier in the southwest, and progressing to the Pacific Northwest and Northern Rocky Mountain region, and finally to the

Mediterranean ecoregions.

The seasonal cycles of temperature, precipitation, and soil moisture reflect both the direct and indirect effects of the seasonal cycle of insolation. In particular,

- the intermonthly changes in temperature are dominated by the insolation variations, but are of lower amplitude in coastal regions;
- the variations in precipitation reflect the influence of two circulation mechanisms, (1) the seasonal variations in the latitude of the westerlies, lower in winter and higher in summer; and (2) the summer monsoon, both driven ultimately by the seasonal cycle of insolation; and
- the variations in soil moisture reflect both moisture availability and evaporative demand, with the broad-scale patterns of intermonthly changes in soil moisture pointing to a greater importance of the latter through most of the year.

Finally, the intermonthly changes in soil moisture provide an explanation for the spatial and temporal variations of fires started by humans and by lightning. For example,

- the locations of the maximum incidence of fire tracks the area in which long-term average soil moisture falls continuously for several months; and
- human-started fires that extend the fire season into winter and early spring occur in regions of generally low soil moisture.

The research described here is part of an effort to examine the within-year variations in the meteorological controls of fire (Hostetler et al. 2003), and interannual and decadal-to-centennial variations of climate and fire, using a combination of climate models, observations (both instrumental and paleoenvironmental), and diagnostic tools.

5. ACKNOWLEDGEMENTS

This research was supported by the Joint Fire Sciences Program (BLMIA 1422RAI01-0040), and by NSF grants ATM-9910638 and ATM-0117160, the US Geological Survey, and the US Environmental Protection Agency
.

6. FURTHER INFORMATION

Further information, including high-resolution versions of Fig. 4, can be found at:
http://geography.uoregon.edu/fireclim/

7. REFERENCES

Bailey, R. G., 1995: Description of the ecoregions of the United States. U.S. Forest Service, Misc. Publication 1381, 108 pp., http://www.fs.fed.us/institute/ecoregions/eco_download.html (accessed August 23, 2003).

Brown, T. J., B. L. Hall, C. R. Mohrle, and H. J. Reinbold, 2002: Coarse assessment of federal wildland fire occurrence data. Desert Research Institute, Program for Climate, Ecosystem and Fire Applications, Report CEFA 02-04, 31 pp., http://www.cefa.dri.edu/Publications/fireoccurrencereport.pdf (accessed August 24, 2003).

Giorgi, F., M. R. Marinucci, and G. T. Bates, 1993: Development of a second-generation regional climate model (RegCM2). Part I: Boundary-layer and radiative transfer processes. *Monthly Weather Review*, **121,** 2794-2813.

Hardy, C. C., K. M. Schmidt, J. P. Menakis, and R. N. Sampson, 2001: Spatial data for national fire planning and fuel management. *International Journal of Wildland Fire*, **10,** 353-372.

Hostetler, S.W., P.J. Bartlein, J.O. Holman, S.L. Shafer, and A.M. Solomon, 2003: Using a regional climate model to diagnose climatological and meterological controls of wildfire in the western United States. *5th Symposium on Fire and Forest Meteorology*, American Meteorological Society, paper P1.3.

Kistler, R., E. Kalnay, W. Collins, S. Saha, G. White, J. Woollen, M. Chelliah, W. Ebisuzaki, M. Kanamitsu, V. Kousky, H. van den Dool, R. Jenne, and M. Fiorino, 2001: The NCEP-NCAR 50-year reanalysis: Monthly means CD-ROM and documentation. *Bulletin of the American Meteorological Society*, **82,** 247-267.

Mitchell, T. D., T. R. Carter, P. D. Jones, M. Hulme, and M. New, 2003: A comprehensive set of high-resolution grids of monthly climate for Europe and the globe: the observed record (1901-2000) and 16 scenarios (2001-2100). *Journal of Climate*, submitted.

Mock, C. J., 1996: Climatic controls and spatial variations of precipitation in the western United States. *Journal of Climate*, **9,** 1111-1125.

Swetnam, T. W. and J. L. Betancourt, 1998: Mesoscale disturbance and ecological response to decadal climatic variability in the American Southwest. *Journal of Climate*, **11,** 3128-3147.

Thompson, S. L. and D. Pollard, 1995: A global climate model (GENESIS) with a land-surface transfer scheme (LSX). Part I: present climate simulation. *Journal of Climate*, **8,** 732-761.

Westerling, A. L., A. Gershunov, T. J. Brown, D. R. Cayan, and M. D. Dettinger, 2003: Climate and wildfire in the western United States. *Bulletin of the American Meteorological Society*, **84,** 595-604.